Dimensionless Study on Efficiency and Speed Characteristics of a Compressed Air Engine

Qihui Yu
School of Automation Science and Electrical Engineering,
Beijing University of Aeronautics and Astronautics,
XueYuan Road No. 37,
HaiDian District,
Beijing 100191, China
e-mail: yqhhxq@163.com

Maolin Cai
School of Automation Science and Electrical Engineering,
Beijing University of Aeronautics and Astronautics,
XueYuan Road No. 37,
HaiDian District,
Beijing 100191, China
e-mail: caimaolin@gmail.com

Yan Shi[1]
School of Automation Science and Electrical Engineering,
Beijing University of Aeronautics and Astronautics,
XueYuan Road No. 37,
HaiDian District,
Beijing 100191, China
e-mail: yesoyou@163.com

Chi Yuan
School of Automation Science and Electrical Engineering,
Beijing University of Aeronautics and Astronautics,
XueYuan Road No. 37,
HaiDian District,
Beijing 100191, China
e-mail: okokok1990@163.com

To eliminate the pollutants exhausting, this paper presents an idea of using compressed air as the power source for engines. Instead of an internal combustion (IC) engine, this automobile is equipped with a compressed air engines (CAEs), which transforms the energy of the compressed air into mechanical kinematic energy. Through analysis of the working process of a CAE, the mathematical model is setup. Experiments are carried out to verify the engine performance and the basic model's validity. By selecting the appropriate reference values, the mathematical model is transformed to a dimensionless expression. The dimensionless speed and efficiency characteristics of the CAE are obtained. Through analysis, it can be obtained that the dimensionless average rotating speed is mainly determined by the intake duration angle, the dimensionless inertia parameter, the dimensionless exhaust pressure, and the scale factor of exhaust valve. Moreover, the efficiency of the CAE is mainly determined by the dimensionless exhaust pressure, the intake duration angle and the dimensionless cylinder clearance. This research can be referred to in the design of CAE and the study on optimization of the CAE.
[DOI: 10.1115/1.4029867]

[1]Corresponding author.

Contributed by the Internal Combustion Engine Division of ASME for publication in the JOURNAL OF ENERGY RESOURCES TECHNOLOGY. Manuscript received July 20, 2014; final manuscript received January 21, 2015; published online March 9, 2015. Assoc. Editor: Avinash Kumar Agarwal.

Keywords: compressed-air engines, average rotating speed, energy efficiency, dimensionless expression

Introduction

Facing the energy crisis and air pollution problem, researches pay more attention to new energy technologies nowadays [1]. It is anticipated that renewable energy may account for 20–30% of the world energy consumption by 2020 [2]. In this situation, the CAE using air as a fuel has attracted much attention over the past decade [3].Compared with the electrical motor, the CAE has unique advantages, such as better safety, lower cost, longer life span, more simple construction, and less pollution during manufacturing process [4]. In the past, the CAE had not been used widely because of its low efficiency, power, and energy density. These days, with the development of carbon–fiber tank technology the air supply pressure of the CAE can be illustrated to 300 bar, and the energy density of the compressed air in the carbon–fiber tank can reach 491.6 kJ/kg [5], which is equal to lithium battery energy density [6].

Previous studies have given different methods to improve CAE's efficiency. Creutzig et al. analyzed the thermodynamic efficiency of a compressed air car powered by a pneumatic engine and considered the merits of compressed air versus chemical storage of potential energy [7]. Huang et al. researched CAE efficiency by experimental investigation [8]. Enhanced heat exchange is an effective method. Williams et al. designed a frost-free cryogenic heat exchangers for automotive propulsion to improve heat exchange coefficient [9]. Known et al. proposed an innovative quasi-isothermal expansion engine [10]. Besides enhancing heat exchange, controlling energy distribution is also an important method. To optimize energy efficiency, MDI designed CAE using a simple electromagnetic distribution system, which controls the flow of air into the engine [11]. But few studies established key influence parameters to energy efficiency, and studies focus on speed characteristics to CAE.

The paper focuses on speed and efficiency characteristics of CAE. To obtain the main parameters which have influence on speed and efficiency characteristics, a dimensionless mathematical model of a CAE is presented, and simulation results are shown and discussed. This research can be referred to in the design of CAEs and the study on optimization of the CAE.

This paper is arranged as follows. First, the working principles of CAE are analyzed in Sec. 2. Second, mathematical models can be setup in Sec. 3. To verified basic mathematical models, experiment is built in Sec. 4. By selecting the appropriate reference values, the basic mathematical model is transformed to a dimensionless expression in Sec. 5. Energy efficiency based on air power is described in Sec. 6. Simulation based on dimensionless mathematical model is performed in Sec. 7. Finally, the conclusions are summarized in Sec. 8.

Introduction of the CAE

Figure 1 shows the structure of a piston-type CAE. For a single cylinder piston-type CAE, its operation is controlled by the valve system (indicated by number 2, number 15, and number 16). The cam (indicated by number 2), which is driven by a crankshaft mechanism and used to trigger the intake and exhaust valves, is retained for fast response of valve moment. In the suction power stroke, the compressed air flows into the cylinder through the intake valve (indicated by number 15), and the piston (indicated by number 5) is driven downward, linear movement of the piston is converted to rotary motion by crank-connecting rod mechanism (indicated by number 6, number 10). The intake valve closes after a specific crank angle; the compressed air inside the cylinder expands and pushes the piston down. When the piston is near the bottom dead center, the exhaust valve opens so that the air with residual pressure discharges under the impetus of the piston. Rotation of the crankshaft (indicated by number 10) is transferred to the valve system by gear train (indicated by number 13, number

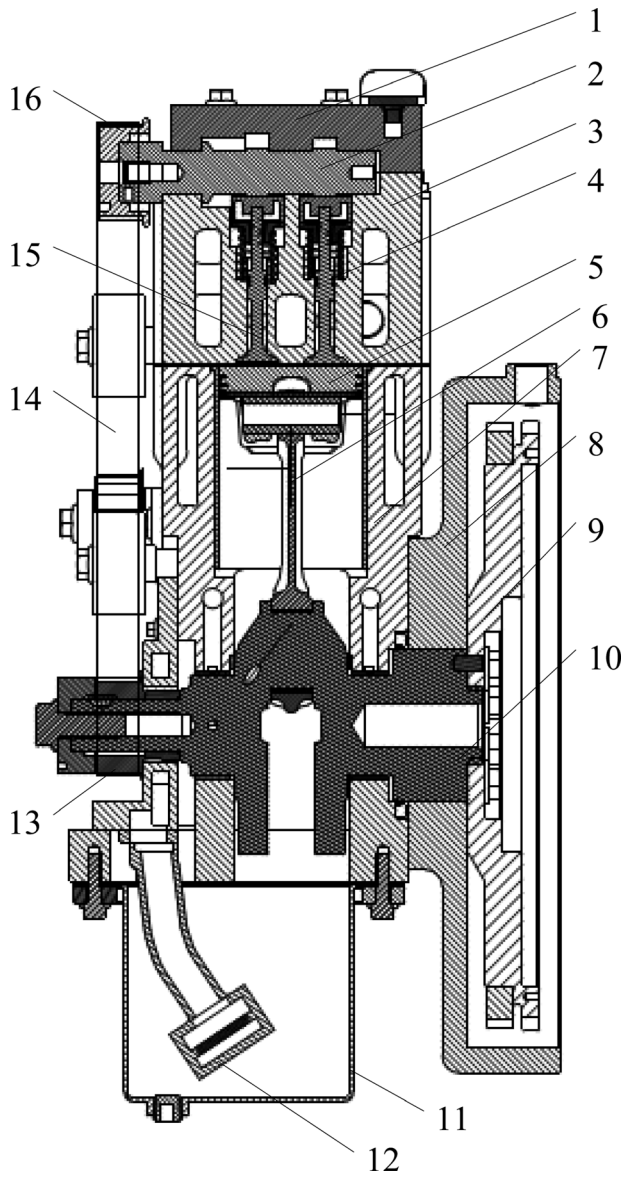

Fig. 1 Structure of the single cylinder CAE

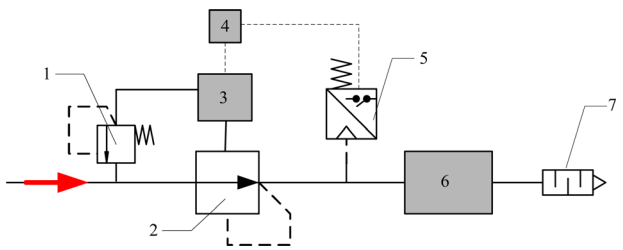

Fig. 2 The ideal schematic diagram of CAE system

14, and number 16). To obtain low friction coefficient, lubrication system (indicated by number 11, number 12) is applied. And flywheel (indicated by number 9) is used to gain smooth speed.

The CAE system, as shown in Fig. 2, consists of a controller, two regulators, an electronic pressure control unit, a CAE, and a Silencer. The major elements and their functions are listed in Table 1. The intake pressure control system consists of a controller (indicated by number 4), two regulators (indicated by number 1 and number 5), an electronic pressure control unit (indicated by number 3), and a pressure sensor (indicated by number 7).

Table 1 The equipment of CAE automobile

Elements	Function
1 Regulator	Regulate gas pressure to meet electronic proportional directional control valve pressure
2 Air operated regulator	Modulate the pressure of entering air and control of CAE
3 Electronic pressure control unit	Modulate the amount of entering air which controls the elements 2
4 Controller	Measure pressure and output the analog signal to the electronic control valve
5 Pressure sensor	Calculate the pressure of airflow
6 CAE	Provide the power
7 Silencer	Reduce exhaust noise

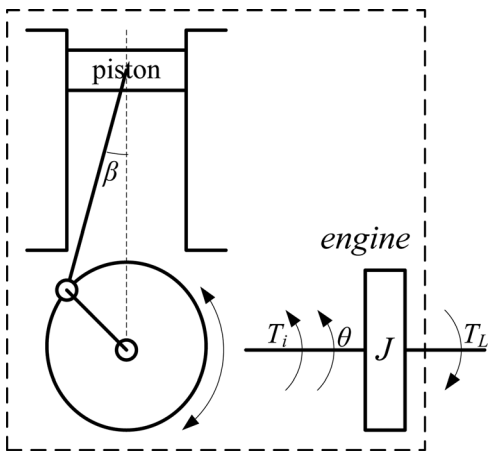

Fig. 3 Engine and load model

Basic Mathematical Models

Figure 3 shows a model of a CAE coupled to a load. The basic thermodynamic mathematical model can be referenced in the author's previous work [12]. The following equation, derived from Newton's principle for a rotation body, describes the dynamics of the system:

$$T_{\mathrm{i}} - T_{\mathrm{r}} - T_{\mathrm{L}} = J\ddot{\theta} \tag{1}$$

The indicated torque (T_{i}) is generated by the conversion of CAE to mechanical energy during the working process. The reciprocating torque (T_{r}) is produced by the motion of the piston assembly and the small end of the connecting rod. T_{L} is load torque. J is the moment of inertia of crankshaft, flywheel, main gear, and rotating part of connecting rod.

The relationship between the pressure inside cylinder (p_{c}), and the indicated torque (T_{i}), can be expressed as

$$T_{\mathrm{i}} = (p_{\mathrm{c}} - p_{\mathrm{a}})A_{\mathrm{p}}rG(\theta) \tag{2}$$

where

$$G(\theta) = \frac{\sin(\theta + \beta)}{\cos\beta} \tag{3}$$

β can be expressed as

$$\beta = \sin^{-1}\frac{r\sin\theta}{L} \tag{4}$$

$$\lambda = r/L \tag{5}$$

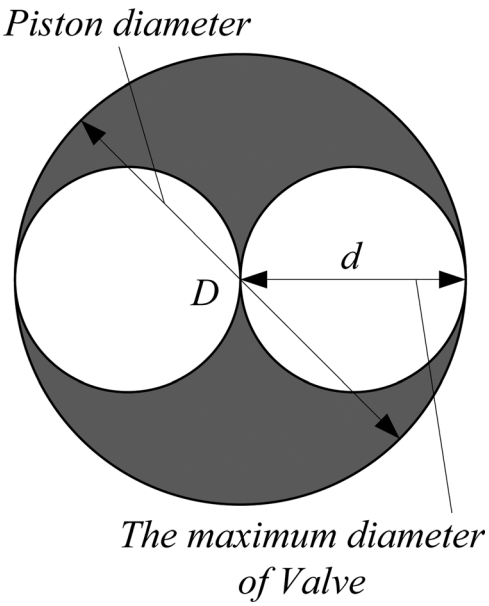

Fig. 4 The relationship between the maximum effective cross-sectional and piston area

From the piston-crank geometry, the piston displacement (y) can be given by

$$y = r + L - L\cos\beta - r\cos\theta \tag{6}$$

The cylinder volume can be given by

$$V(\theta) = \frac{\pi D^2}{4} y(\theta) + V_c \tag{7}$$

The reciprocating torque (T_r), is given by

$$T_r = MrG(\theta)(\cos\theta + \lambda\cos 2\theta)\dot{\theta}^2 \tag{8}$$

According to road performance, the load torque can be expressed as

$$T_L = C_1\dot{\theta}^2 + C_2\ddot{\theta} \tag{9}$$

where C_1 is resistance parameter during the operation process, C_2 is resistance parameter during the acceleration process.

The effective sectional area of the intake and exhaust valve can be expressed as

$$A_1 = \begin{cases} \tau_1 A_{e\max} & 0 \le \theta < \theta_1 \\ 0 & \text{others} \end{cases} \tag{10}$$

$$A_2 = \begin{cases} \tau_2 A_{e\max} & pi \le \theta < \theta_2 \\ 0 & \text{others} \end{cases} \tag{11}$$

If some extra area for support material around the valves is not considered, the maximum diameter of intake or exhaust valve can be illustrated by Fig. 4.

According to Fig. 4, the maximum effective area can be expressed as

$$A_{e\max} = \frac{\pi D^2}{16} \tag{12}$$

Table 2 Major structural parameters of the verification prototype

Type	Specification
Number of cylinder	1
Bore × Stroke	88.0 mm × 89.0 mm
Displacement	400 cc
Crank-link rod ratio	0.316
Compression ratio	9.5
Intake valve lift	6.4 mm
Exhaust valve lift	6.4 mm
Intake valve opening	0 deg (crank angle)
Intake valve closing	130 deg (crank angle)
Exhaust valve opening	180 deg (crank angle)
Exhaust valve closing	340 deg (crank angle)

Experimental Study on the CAE System

To verify the feasibility of the CAE, a prototype was modified from a single cylinder piston-type IC engine by transforming its valve system. Major structural parameters of the prototype are shown in Table 2.

The test platform, as seen in Fig. 5, consists of a regulator, a tank, a cylinder pressure sensor (4075A, KISTLER), an intake pressure sensor, a coupling, an eddy current dynamometer, a reformed CAE and a data acquisition system. The compressed air, discharged from an air tank, flows through the pipeline, and into the CAE.

The test bench was designed to measure the CAE's operating parameters and performances, including intake pressure, rotating speed, torque of the CAE. The pressure transducer was installed at the inlet pipe of the CAE to measure inlet pressure. The cylinder pressure sensor was installed at the cylinder head to measure the pressure inside cylinder of the CAE.

Curves of output torque and output power variation in different intake pressure at 300 rpm rotating speed are shown in Fig. 6, curves of cylinder pressure are shown in Fig. 7.

As shown in Fig. 6, the output torque and power of the CAE are measured by the experimental bench at various supply pressure and 300 rpm rotating speed. The experimental and simulation results have similar trends. Both torque and power curves increase with the supply pressure at constant rotate speed. The torque and power of the simulation results are higher than the experimental results at same supply pressure, and the errors will increase with the supply pressure. This is because compressed air leakage will happen during the CAE operation and the leakage will be acuter with the supply pressure.

The pressure curve of the compressed air in the cylinder is shown in Fig. 7. It is clear that the simulation results are consistent with the experimental results, and that verifies the mathematical model above. The cylinder pressure can be obtained by the simulation, as shown in Fig. 7. The experimental and simulation curves have similar trends. The main reasons for the difference between the simulation results and the experimental results are the fluctuation of the supply pressure, leakage between piston and cylinder and the friction.

Dimensionless Mathematical Model

To obtain main influence parameters on efficiency and speed, further research on its speed and efficiency characteristics is essential. In this section, a dimensionless mathematical model of the CAE is proposed. The reference values and the dimensionless variables are shown in Table 3. The basic mathematical can be made dimensionless as described in the Dimensionless Energy Equation section.

Dimensionless Energy Equation. The dimensionless energy equation is described by

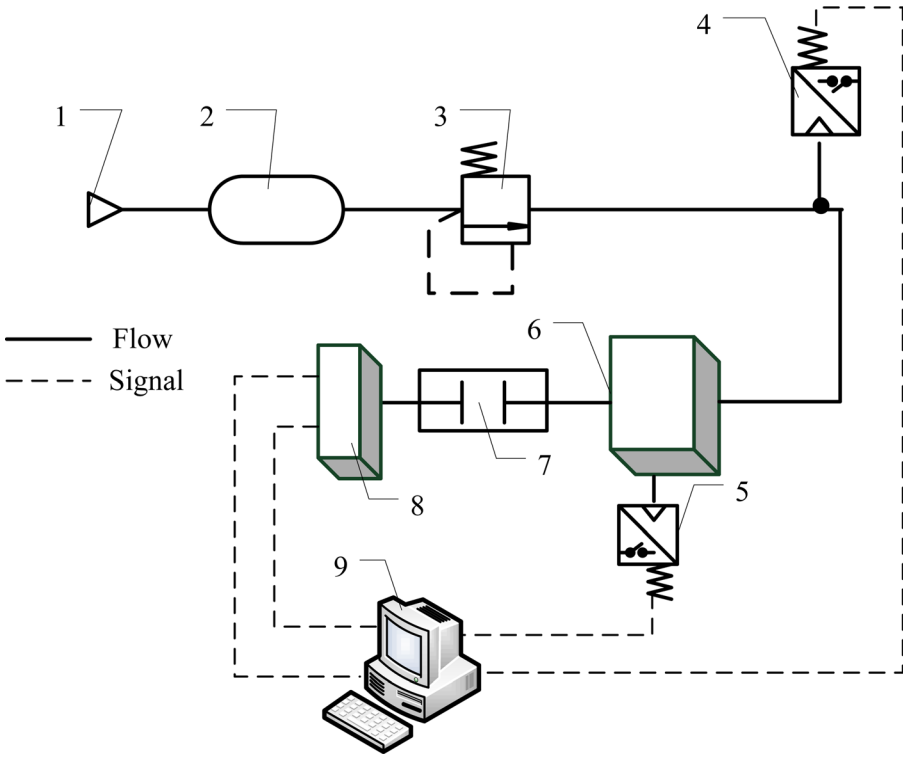

Fig. 5 Configuration of experimental apparatus: (1) compressor, (2) buffer bank, (3) pressure regulator, (4) intake pressure sensor, (5) cylinder pressure sensor, (6) CAE, (7) coupling, (8) eddy current dynamometer, and (9) data acquisition system

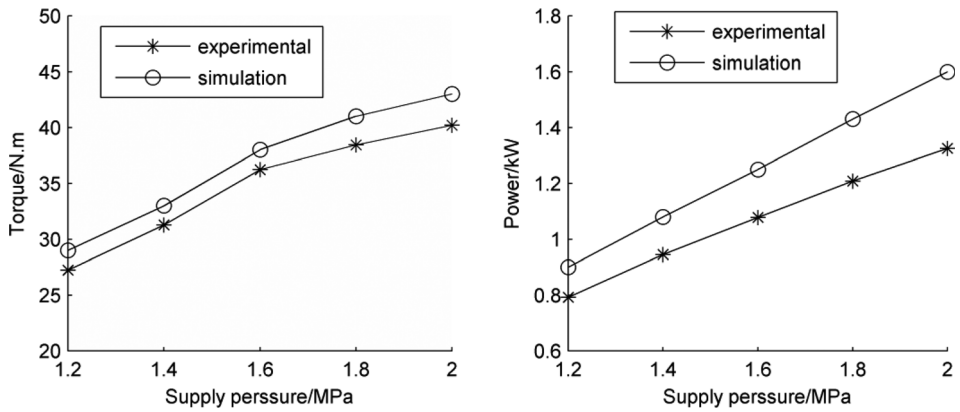

Fig. 6 Curves of output torque, output power variation in different intake pressure

$$\frac{dT^*}{dt^*} = \frac{1}{m^*}\left[t^*_{hc}A^*_h(1-T^*) - (\kappa-1)T^*G^*_2 + \kappa T^*_1 G^*_1 - (\kappa-1)\frac{p^*dV^*}{dt^*} - T^*G^*_1\right] \tag{13}$$

where the dimensionless parameter (t^*_{hc}), which is the dimensionless temperature settling time of the cylinder, is the ratio of the temperature settling time constant (t_{hc}), and the time reference value (t_b) [13]. The dimensionless and dimensional time constant can be written as follows:

$$t^*_{hc} = \frac{t_{hc}}{t_b} \tag{14}$$

$$t_{hc} = \frac{C_v m_b}{aA_b} \tag{15}$$

$$A^*_h = 2 + 4\frac{y^*}{D^*} \tag{16}$$

Dimensionless Equation of Continuity. The dimensionless equation of continuity can be given as the following equation:

$$\frac{dm^*}{dt^*} = G^* \tag{17}$$

Dimensionless Flow Equation. The dimensionless flow equation is

$$G^* = \begin{cases} \tau_i \dfrac{B}{H}\dfrac{p^*_u}{\sqrt{T^*_u}}\sqrt{\left(\dfrac{p^*_d}{p^*_u}\right)^{\frac{2}{\kappa}} - \left(\dfrac{p^*_d}{p^*_u}\right)^{\frac{\kappa+1}{\kappa}}} & \dfrac{p^*_d}{p^*_u} > 0.528 \\ \tau_i \dfrac{p^*_u}{\sqrt{T^*_u}} & \dfrac{p^*_d}{p^*_u} \le 0.528 \end{cases} \tag{18}$$

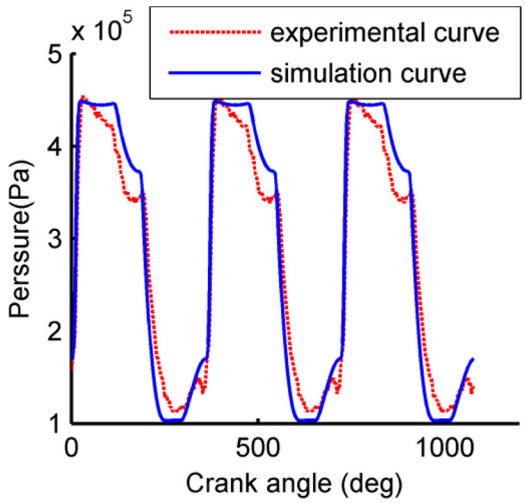

Fig. 7 Curves of cylinder pressure

where

$$B = \sqrt{\frac{2\kappa}{R(\kappa-1)}} \tag{19}$$

$$H = \left(\frac{2}{\kappa+1}\right)^{\frac{1}{\kappa-1}} \sqrt{\frac{2\kappa}{R(\kappa-1)}} \tag{20}$$

Dimensionless Dynamic Equation. The dimensionless dynamic equation can be written as follows:

$$\frac{d^2\theta}{d(t^*)^2} = \left(\frac{1}{t_f^*}\right)^2 (p^* - p_a^*)G(\theta) - \varepsilon\left[(\cos\theta + \lambda\cos 2\theta)\dot{\theta}^2\right]G(\theta) - \frac{1}{t_L^*}\left[C_1^*\left(\frac{d\theta}{dt^*}\right)^2 + C_2^*\frac{d^2\theta}{d(t^*)^2}\right] \tag{21}$$

Referred to J-parameter that is used in the current selection method of a pneumatic cylinder [14,15], dimensionless inertia parameter (t_f^*), is defined in the following equation:

$$t_f^* = \frac{t_f}{t_b} \tag{22}$$

$$t_f = \sqrt{\frac{J/r}{p_s A_p}} \tag{23}$$

where ε is the ratio of the moment of inertia, which is defined in the following equation:

$$\varepsilon = \frac{M_i r^2}{J} \tag{24}$$

where, C_1^* and C_2^* which can be written as follows:

$$C_1^* = \frac{C_1}{p_s A_p} \tag{25}$$

$$C_2^* = \frac{C_2}{p_s A_p} \tag{26}$$

Dimensionless State Equation. The dimensionless state equation can be expressed by

$$p_c^* V^* = m^* T^* \tag{27}$$

Efficiency Analysis

There are two ways to evaluate the efficiency of the CAE. One is the overall efficiency which takes account of compressed air production, storage, transport and transformation into mechanical energy. The other is the operational efficiency which is useful in the design, optimization, and evaluation of a CAE. In this paper, the efficiency is the operational efficiency. There are two ways to define energy efficiency in current research. One is the ratio of the output shaft energy to the input energy of the CAE as follows [8]:

$$\eta = \frac{2\pi n T_{or}}{\Delta p Q} \tag{28}$$

The other way is shown as follows [16]:

$$\eta = \frac{2\pi n T_{or}}{p_s Q} \tag{29}$$

According to Ref. [17], the available energy of compressed air can be calculated as follows:

$$E = m_s R T_a \left[\ln\frac{p_s}{p_a} + \frac{\kappa}{\kappa-1}\left(\frac{T_1}{T_a} - 1 - \ln\frac{T_1}{T_a}\right)\right] \tag{30}$$

Dimensionless available energy becomes

$$E^* = m_s^*\left[\ln\frac{1}{p_a^*} + \frac{\kappa}{\kappa-1}\left(T_1^* - 1 - \ln T_1^*\right)\right] \tag{31}$$

Table 3 Reference values and dimensionless variables

Variable	Reference value	Dimensionless variable
Displacement	S Stroke	$x^* = x/S$
Area of piston	A_p Area of piston	$A^* = A/A_p$
Volume	$V_b = A_p \cdot S$	$V^* = V/V_b$
Pressure	p_s Supply pressure	$p^* = p/p_b$
Temperature	T_a Atmosphere temperature	$T^* = T/T_a$
Air mass flow	$G_{max} = \frac{A_{e\,max} p_s C}{\sqrt{T_a}}$ Maximum air mass flow	$G^* = G/G_{max}$
Air mass	$m_b = \frac{p_s V_b}{R T_a}$	$m^* = m/m_b$
Time	$t_b = \frac{m_b}{G_b} \frac{V_b}{A_{e\,max} C R \sqrt{T_a}}$	$t^* = t/t_b$
Work	$W_b = p_s V_b$	$W^* = W/W_b$
Power	$P_b = W_b/t_b$	$P^* = P/P_b$
Torque	$T_b = p_b V_b/2\pi$	$T_{or}^* = T_{or}/T_b$

Table 4 The initial values of the parameters

Parameter	V_c^*	λ	D^*	τ_1	τ_2
Value	0.1	0.314	1	0.25	0.5
Parameter	T_1^*	p_a^*	t_{hc}^*	θ_1	θ_2
Value	1	0.05	0.0001	pi/3	11*pi/6
Parameter	t_f^*	ε	C_1^*	C_2^*	
Value	2.5	0.06	0.0001	0.0001	

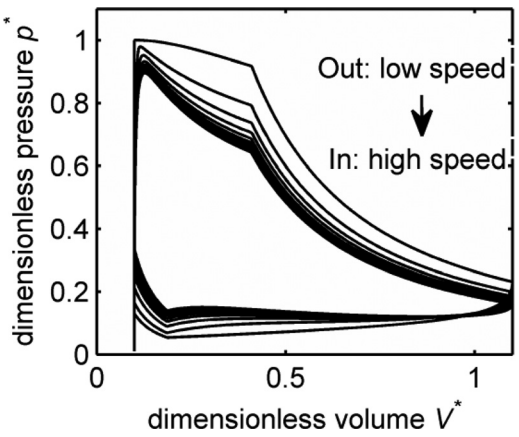

Fig. 8 Working cycle for CAE

In a working cycle, the output work of the CAE can be expressed as

$$W = \int p dV \tag{32}$$

The dimensionless output work becomes

$$W^* = \int p^* dV^* \tag{33}$$

The energy efficiency of the CAE can be calculated as follows:

$$\eta = \frac{E^*}{W^*} \tag{34}$$

Simulations and Analysis

From the discussion above, it can be obtained that the dimensionless speed and efficiency are determined by 14 dimensionless parameters. The initial values of the 14 dimensionless parameters are shown in Table 4. The software, MATLAB/SIMULINK, is used for modeling the simulation. Figure 8 shows the working cycle for CAE. Figure 9 depicts the dimensionless speed and efficiency characteristics of CAE.

From Fig. 8, the relationship between dimensionless volume and dimensionless pressure are obtained. At the beginning of the movement, because the driving torque is larger than the load torque, the rotation speed increases. At this time, the pressure inside cylinder is stable during intake compressed air process. With the increase of rotation speed, the mass of compressed air will enter the cylinder, and the pressure inside cylinder will reduce, and lead driving torque decreasing until a stable working cycle.

Thermodynamically, the working process of the CAE can be considered to be the reverse process of the piston-type air compressor. The CAE loss consists of adiabatic expansion loss, intake process loss, and exhaust process loss. The energy loss will increase with the working crankshaft speed.

Figure 9(*a*) shows the dimensionless rotating speed of crankshaft during the working process. When the average

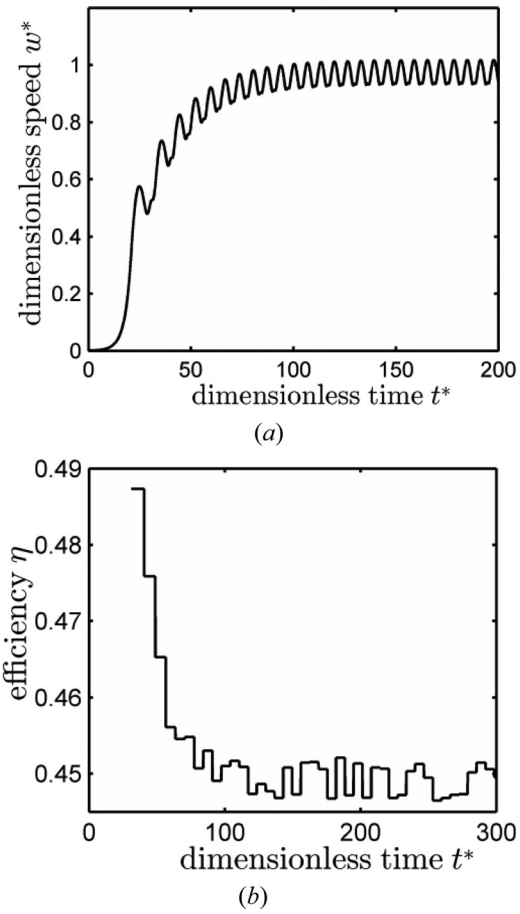

Fig. 9 Speed and efficiency characteristics of CAE

dimensionless output torque is equal to the dimensionless load torque, the average speed tends to stabilize. Figure 9(*b*) shows the energy efficiency variation curve during the working process. Because the energy loss will increase when the dimensionless rotating speed of crankshaft increases, the energy efficiency will decrease. The dimensionless rotating speed fluctuation leads to the energy efficiency fluctuation.

As is known, C_1^* and C_2^* are resistance parameters which cannot be controlled, the relationship between resistance parameters and speed, efficiency characteristics is not considered in this paper.

According to the mathematical model above, each dimensionless parameter can be changed for comparison while all other dimensionless parameters are kept constant. To evaluate speed and efficiency characteristics of the CAE, the average dimensionless rotating speed of crankshaft and efficiency are defined as

$$\overline{\omega^*} = \frac{\int_0^t \omega^* dt}{t} \tag{35}$$

$$\overline{\eta} = \frac{\int_0^t \eta dt}{t} \tag{36}$$

The change rate of the dimensionless rotating speed is the ratio of the change in the dimensionless average rotating speed for one parameter and the total change ($\overline{\omega}_{\text{total-cg}}$) in the dimensionless average rotating speed for all parameters. The rate of changes of the dimensionless average rotating speed for the ratio of crank radius and connecting rod link length is given by Eq. (39)

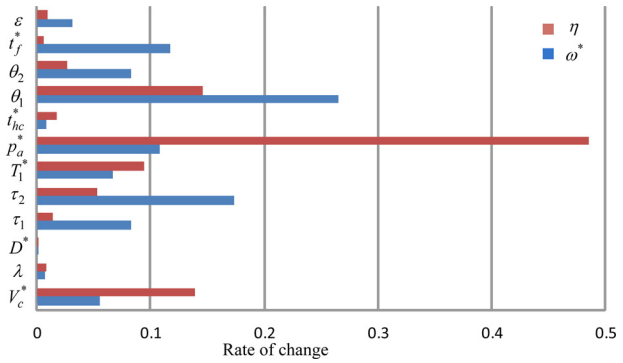

Fig. 10 Rate of change of speed and efficiency for each parameter

$$\overline{\omega_{\text{total-cg}}} = \overline{\omega_{V_c^*-\text{cg}}} + \overline{\omega_{\lambda-\text{cg}}} + \overline{\omega_{D^*-\text{cg}}} + \overline{\omega_{\tau_1-\text{cg}}} + \overline{\omega_{\tau_2-\text{cg}}} + \overline{\omega_{T_1^*-\text{cg}}} + \overline{\omega_{p_a^*-\text{cg}}} + \overline{\omega_{t_{hc}^*-\text{cg}}} + \overline{\omega_{t_f^*-\text{cg}}} + \overline{\omega_{\varepsilon-\text{cg}}} + \overline{\omega_{\theta_1-\text{cg}}} + \overline{\omega_{\theta_2-\text{cg}}} \quad (37)$$

$$\overline{\omega_{\lambda-\text{cg}}} = \frac{\overline{\omega_{\lambda-\max}} + \overline{\omega_{\lambda-\min}}}{\lambda_{\text{av}}} \quad (38)$$

$$n_\lambda = \frac{\overline{\omega_{\lambda-\text{cg}}}}{\overline{\omega_{\text{total-cg}}}} \quad (39)$$

where λ_{av} is the average value of the ratio of crank radius and connecting rod link length change.

The rate of change of efficiency is the ratio of the change in the efficiency for one parameter and the total change ($\overline{\omega_{\text{total-cg}}}$) in the efficiency for all parameters, which is defined with the method mentioned above.

Figure 10 describes the rate of change of the dimensionless rotating speed of crankshaft for each parameter.

It can be seen from Fig. 10 that:

(a) The dimensionless average rotating speed is influenced significantly by the dimensionless inertia parameter (t_f^*) the intake duration angle (θ_1), the dimensionless exhaust pressure (p_a^*), and the scale factor of exhaust valve (τ_2). The rates of changes of the average rotating speed for the four parameters are 0.1168, 0.2652, 0.108, and 0.1738, respectively.
(b) The dimensionless average rotating speed is slightly affected by the dimensionless temperature settling time (t_{hc}^*), the dimensionless piston diameter (D^*), and the ratio of the crankshaft radius and link length (λ).
(c) The energy efficiency is influenced significantly by the dimensionless exhaust pressure (p_a^*), the intake duration angle (θ_1), and the dimensionless cylinder clearance (V_c^*). The rates of changes of the efficiency for the three parameters are 0.4857, 0.1457, and 0.1394, respectively.
(d) The energy efficiency is hardly affected by the dimensionless inertia parameter (t_f^*), the moment of inertia ratio (ε), the dimensionless temperature settling time (t_{hc}^*), the scale factor of intake valve (τ_1), the dimensionless piston diameter (D^*), and the ratio of the crankshaft radius and link length (λ).

In summary, the dimensionless rotating speed and energy efficiency are mainly determined by the dimensionless inertia parameter, the intake duration angle, the dimensionless exhaust pressure, the scale factor of exhaust valve, and the dimensionless cylinder clearance. The other parameters can be neglected, so the

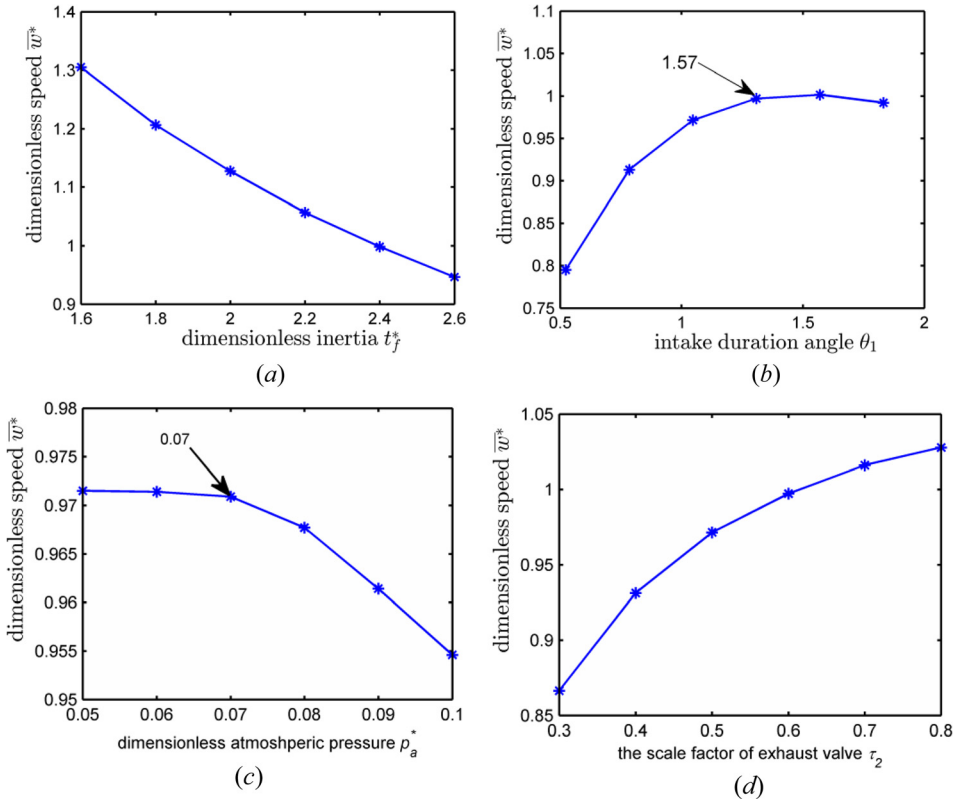

Fig. 11 Rotating speed characteristics of the CAE. (*a*) Relationship between rotating speed and t_f^*, (*b*) relationship between speed and θ_1, (*c*) relationship between rotating speed and p_a^*, and (*d*) relationship between speed and τ_2.

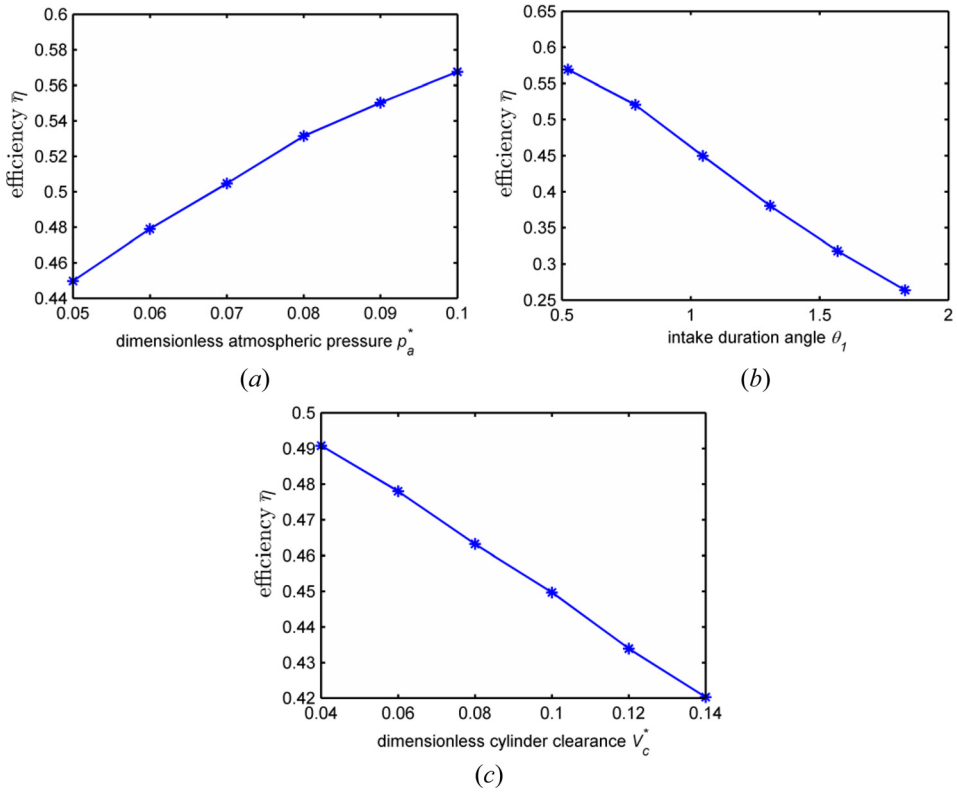

Fig. 12 Efficiency characteristics of the CAE. (*a*) Relationship between efficiency and p_a^*, (*b*) relationship between efficiency and θ_1, (*c*) relationship between efficiency and V_c^*.

study on optimization of the CAE can be carried on based on the analysis of the influence of the five dimensionless parameters on the dimensionless average rotating speed and the efficiency.

The relationship between the dimensionless rotating speed and the dimensionless inertia parameter, the intake duration angle, the dimensionless exhaust pressure, and the scale factor of exhaust valve were studied, and results are shown in Fig. 11. The relationship between the energy efficiency and the dimensionless exhaust pressure, the intake duration angle, and the dimensionless cylinder clearance were studied, and the results are shown in Fig. 12.

From Figs. 11 and 12, it can be seen that:

(a) The dimensionless average rotating speed decreases with an increase in the dimensionless inertia parameter. The reason is that the growth of the dimensionless parameters represents the increase of moment of inertia of crankshaft, flywheel, main gear, and rotating of connecting rod.
(b) The dimensionless average rotating speed increases with the intake duration angle. When the intake duration angle is bigger than 1.57, the dimensionless average rotating speed remains almost constant.
The primary reason is that when the intake duration angle is lower than 1.57, flowing into the cylinder the mass of compressed air decreases. That will reduce the output torque and the rotating speed. However, if the intake duration angle is bigger than 1.57, the compressed air in the cylinder is not completely discharged. This leads to a higher pressure in the cylinder and the pressure blocks the motion of the piston and reduces the rotating speed since it's often higher than the atmospheric pressure.
(c) When the dimensionless exhaust pressure is lower than 0.07, the dimensionless rotating speed remains almost constant; when the dimensionless exhaust pressure is higher than 0.07, the dimensionless average rotating speed starts to decrease sharply.
(d) The dimensionless average rotating speed increases with the scale factor of exhaust valve.
That is because when the scale factor of the exhaust valve increases, the compressed air in the cylinder is easy to be discharged.
(e) The average efficiency increases with an increase in the dimensionless exhaust pressure. The main reason is that, when the dimensionless exhaust pressure increases, the compressed air power can be fully expanded.
(f) The average efficiency decreases with an increase in the intake duration angle. That is because that, the bigger the intake duration angle is, the more the compressed air flows into the cylinder. However, the compressed air in the cylinder is not completely expanded.
(g) The average efficiency decreases with an increase in the dimensionless cylinder clearance. The main reason is that, the bigger the cylinder clearance is, the more the compressed air flows in to the cylinder. Note that the compressed air in the cylinder clearance does not produce energy output.

Conclusions

In this paper, a CAE system was introduced, and the working process of the CAE was studied. The basic model was verified by experiment. Based on the mathematical model in previous study, appropriate reference values were selected. Then the dimensionless model of the CAE was proposed, and the dimensionless rotating speed and efficiency were analyzed with simulation. The conclusions are summarized as follows:

(1) Simulation results have consistency with experimental results, and that proves the mathematical model of the CAE is correct.
(2) The dimensionless average rotating speed characteristics of the CAE are mainly determined by the dimensionless

inertia parameter, the intake duration angle, the dimensionless exhaust pressure, and the scale factor of exhaust valve. The influence of all other parameters on the dimensionless average rotating speed can be neglected.

(3) The energy efficiency characteristics of the CAE are mainly determined by the dimensionless exhaust pressure, the intake duration angle and the dimensionless cylinder clearance. The influence of all other parameters on the energy efficiency can be neglected.

(4) When the intake duration angle is smaller than 1.57, the dimensionless average rotating speed increases with the intake duration angle. When the intake duration angle is bigger than 1.57, the dimensionless average rotating speed remains almost constant.

(5) When the dimensionless exhaust pressure is lower than 0.07, the dimensionless rotating speed remains almost constant. When the dimensionless exhaust pressure is higher than 0.07, the dimensionless average rotating speed decreases sharply with an increase in the dimensionless exhaust pressure.

This research can be referred in the design of CAE system and the study on optimization of the CAE system.

Nomenclature

A_h = heat transfer area (m^2)
A_p = piston area (m^2)
A_{emax} = the maximum effective cross-sectional area (m^2)
C_1,C_2 = coefficients
D = cylinder bore diameter (m)
E = air power (J)
G = air mass flow (kg/s)
J = the moment of inertia of crankshaft, flywheel, main gear and rotating part of connecting rod ($kg \cdot m^2$)
L = connecting rod length (m)
m = air mass (kg)
M = piston, rings, pin, and small end of connecting rod mass (kg)
n = rotating speed (rpm)
P = output power (w)
p_a = atmospheric pressure (=101 kPa)
p_c = cylinder pressure (Pa)
p_s = supply pressure (Pa)
Q = airflow value under compressed condition (cm^3/s)
r = crank radius (m)
R = gas constant
S = stroke (m)
t = time (s)
T = temperature (K)
T_i = indicated torque (N·m)
T_L = load torque (N·m)
T_r = reciprocating torque (N·m)
T_{or} = torque of the CAE (N·m)
V_c = cylinder clearance (m^3)
W = output work (J)
β = connecting rod angle (rad)
Δp = different pressure from inlet to outlet (kg f/cm^2)
η = efficiency
θ = crankshaft angular position (rad)
θ_1 = intake duration angle (rad)
θ_2 = exhaust duration angle (rad)
κ = specific heat ratio (=1.4)
λ = the ratio of crank radius and connecting rod length
τ_1, τ_2 = scale factor of intake valve and exhaust valve
ω = angle speed (rad/s)

Subscripts

b = reference value
c = inside cylinder
d = downstream side
s = supply
u = upstream side
1 = intake
2 = exhaust

Superscript

* = dimensionless

References

[1] Shafiee, S., and Topal, E., 2009, "When Will Fossil Fuel Reserves be Diminished?," Energy Policy, **37**(1), pp. 181–189.
[2] Gadonneix, P., Sambo, A., Nadeau, M.-J., Statham, B. A., Kim, Y. D., Birnbaum, L., Vargas Lleras, J. A., Cho, H., Ward, G., Arup Roy Choudhury, A. R., Wu, X., da Costa Carvalho Neto, J., Zatari, T. M., Dauger, J.-M., Frei, C., and Meyers, K., 2013, "World Energy Resources 2013 Survey." Available at: http://www.worldenergy.org/publications/2013/world-energy-resources-2013-survey/
[3] Chen, Y., Xu, H., Tao, G. L., Wang, X. Y., Liu, H., and Jia, G. Z., 2002, "Research and Progress of the Compressed Air Power Vehicle," Chin. J. Mech. Eng., **38**(11), pp. 7–12.
[4] Zhang, Y., and Nishi, A., 2003, "Low-Pressure Air Motor for Wall-Climbing Robot Actuation," Mechatronics, **13**(4), pp. 377–392.
[5] Chen, H., Ding, Y., Li, Y., Zhang, X., and Tan, C., 2011, "Air Fuelled Zero Emission Road Transportation: A Comparative Study," Appl. Energy, **88**(1), pp. 337–342.
[6] Ibrahim, H., Ilinca, A., and Perron, J., 2008, "Energy Storage Systems-Characteristics and Comparisons," Renewable Sustainable Energy Rev., **12**(5), pp. 1221–1250.
[7] Creutzig, F., Papson, A., Schipper, L., and Kammen, D. M., 2009, "Economic and Environmental Evaluation of Compressed-Air Cars," Environ. Res. Lett., **4**, p. 044011.
[8] Huang, C.-Y., Hu, C.-K., Yu, C.-J., and Sung, C.-K., 2013, "Experimental Investigation on the Performance of a Compressed-Air Driven Piston Engine," Energies, **6**(3), pp. 1731–1745.
[9] Williams, J., Knowlen, C., Mattick, A. T., and Hertzberg, A., 1997, "Frost-Free Cryogenic Heat Exchanges for Automotive Propulsion," AIAA Paper No. 97-3168.
[10] Known, C., Williams, J., Mattick, A. T., Deparis, H., and Hertzberg, A., 1997, "Quasi-Isothermal Expansion Engines for Liquid Nitrogen Automotive Propulsion," SAE Paper No. 972649.
[11] Thipe, S. S., 2008, "Compressed Air Car," Special Feature: Air Pollution Control Technologies. Available at: http://www.techmonitor.net/tm/images/1/18/08nov_dec_sf4.pdf
[12] Yu, Q., Cai, M., Shi, Y., and Fan, Z., 2014, "Optimization of the Energy Efficiency of a Piston Compressed Air Engine," Strojniški vestnik-J. Mech. Eng., **60**(6), pp. 395–406.
[13] Kagawa, T., 1985, "Heat Transfer Effects on the Frequency Response of a Pneumatic Nozzle Flapper," ASME J. Dyn. Syst. Meas. Control, **107**(4), pp. 332–336.
[14] Singh, B. R., and Singh, O., 2008, "Development of a Vaned-Type Novel Air Turbine," Proc. Inst. Mech. Eng., Part C, **222**(12), pp. 2419–2426.
[15] Shi, Y., and Cai, M., 2013, "Dimensionless Study on Output Flow Characteristics of Expansion Energy Used Pneumatic Pressure Booster," ASME J. Dyn. Syst. Meas. Control, **135**(2), p. 021007.
[16] Shen, Y.-T., and Hwang, Y.-R., 2009, "Design and Implementation of an Air-Powered Motorcycles," Appl. Energy, **86**(7–8), pp. 1105–1110.
[17] Cai, M., Kawashima, K., and Kagawa, T., 2006, "Power Assessment of Flowing Compressed Air," ASME J. Fluids Eng., **128**(2), pp. 402–405.